Band alignments of sputtered dielectrics on GaN

S.N. Supardan[1,2,a], P. Das[3,a,*], J.D. Major[4], A. Hannah[5], Z.H. Zaidi[6], R. Mahapatra[3,*], K.B. Lee[6], R. Valizadeh[5], P.A. Houston[6], S. Hall[1], V.R. Dhanak[4], and I.Z. Mitrovic[1,*]

[1]Dept. of Electrical Engineering & Electronics, University of Liverpool, Liverpool L69 3GJ, UK

[2]Dept. of Physics and Material Studies, Universiti Teknologi MARA, 40450 Shah Alam, Selangor, Malaysia

[3]Dept. of Electronics & Communication Engineering, National Institute of Technology Durgapur, Durgapur 713209, India

[4]Dept. of Physics and Stephenson Institute for Renewable Energy, University of Liverpool, Liverpool L69 7ZF, UK

[5]ASTeC Vacuum Science Group, STFC Daresbury Laboratory, Cheshire WA4 4AD, UK

[6]Dept. of Electronic and Electrical Engineering, University of Sheffield, Sheffield S1 3JD, UK

[*] Electronic mail of the corresponding author: partha.das@liverpool.ac.uk; pd.16ec1103@phd.nitdgp.ac.in; rajat.mahapatra@ece.nitdgp.ac.in; ivona@liverpool.ac.uk

[a] S.N. Supardan and P. Das have contributed equally to this work.

Abstract

The band alignments of sputtered ZrO_2, Al_2O_3 and MgO on GaN have been measured experimentally using X-ray photoelectron spectroscopy (XPS). The valence band offsets (± 0.2 eV) for ZrO_2, Al_2O_3 and MgO on GaN using Kraut's method and charge-corrected XPS core levels were found to be 0.4 eV, 1.1 eV and 1.2 eV with corresponding conduction band offsets (± 0.2 eV) of 1.3 eV, 2.0 eV and 2.8 eV, respectively. The electrical characterization of Metal Insulator Semiconductor (MIS)-capacitors with different gate dielectrics (ZrO_2, Al_2O_3 and MgO) has been performed as well. The current density of the MIS-capacitors with gate dielectrics MgO and Al_2O_3 at a positive bias of 1 V show lower leakage currents of 3.2×10^{-6} A/cm^2 and 5.3×10^{-6} A/cm^2 respectively, whereas, the MIS-capacitors with ZrO_2 gate dielectric have the highest leakage current of 6.2×10^{-4} A/cm^2 at 1 V.

Keywords: Gallium nitride, dielectrics, X-ray photoelectron spectroscopy, band offsets, Kraut's method, metal-insulator-semiconductor.

1. Introduction

GaN based power devices, especially high electron mobility transistors (HEMTs), have been demonstrated over the past few decades. The devices have the potential to satisfy the ever-growing demand for improved performance in terms of speed, power and efficiency. The HEMT has the advantages of offering simple associated circuit design and fail-safe operation [1–4]. GaN devices are particularly suited to high power switching applications due to their unique and valuable material properties; including wide band gap (3.4 eV), high electron saturation velocity (3×10^7 cm/s) and high critical breakdown electric field (4.2 MV/cm) [5]. Currently the GaN based Metal-Insulator-Semiconductor (MIS)-HEMT device is seen to demonstrate superior performance in power electronics applications over the Schottky gate counterpart, due to its inherently lower gate leakage current [6], together with the ability to provide larger forward gate voltage swing by engineering the threshold voltage (V_{th}) between depletion and enhancement mode operation [7] and also an improved gate-drain breakdown voltage [8].

However, introduction of high-k gate dielectric layer may also affect the device performance such as leakage current, lower channel mobility and threshold voltage instability. High band gap gate dielectric materials are preferable as they can provide higher tunnelling barriers for electrons and holes, which result in lower gate leakage current. On the other hand, high dielectric constant (high-k) material is also necessary for improved electrostatic control over the channel and improved on-current, which in-turn results in higher transconductance. The quality of the gate dielectric and the dielectric/GaN interface also plays a central role in device performance due to potential problems arising from fixed oxide charge, border and interface traps (fast and slow states). The origin of interface traps may be due to structural damage, oxidation induced defects or dangling bonds [9]. The dynamic charging and discharging of the trap states leads to threshold voltage instability, large hysteresis and significant current collapse [10] which affect the switching performance. Proper selection of high-k dielectric materials based on the aforementioned criteria is mandatory. Materials such as SiN [11–13] and Al_2O_3 [12,14] have been used in an attempt to passivate the interface, however high interface state densities (D_{it}) of ~3×10^{12} $cm^{-2}eV^{-1}$ [11] and 3.4×10^{12} $cm^{-2}eV^{-1}$ [12], respectively have been reported. Atomic layer deposition (ALD) of Al_2O_3 [15–17] is the most commonly used gate dielectric deposition process. Alumina offers a large band offset with GaN material, high dielectric constant ($k \sim 8.6 – 10$), high breakdown electric field (~ 10 – 30 MV/cm) and good interface quality with an average D_{it} of ~7×10^{10} $cm^{-2}eV^{-1}$ and a

corresponding hysteresis voltage of 100 mV [18]. Regarding the investigation of band offset between high-k gate dielectrics and III-V substrate, several publications have been reported [19-22]. In 2012, Yang *et al.* [15] reported a large valence band offset (VBO) of 1.8 eV for plasma-enhanced (PE)-ALD deposited Al_2O_3 on HCl-treated n-type GaN. In this work, the theoretical value of 17.8 eV was used as the binding energy (BE) of Ga 3d X-ray photoelectron spectroscopy (XPS) core level (CL) below the valence band maximum (VBM) for the calculation of VBO by Kraut's method [23]. The combination of XPS and ultraviolet photoemission spectroscopy (UPS) data in [15] gave an indication of a strong upward band bending at 1 nm Al_2O_3/n-GaN. It has been shown that spontaneous polarization in GaN results in a surface bound charge, which has been found to be negative in the case of the Ga-face GaN [24]. Thus, a compensating space charge region comprising positive donors forms near the surface, depleting the n-type GaN [25], and resulting in a strong upward band bending (BB) of ~0.9 eV for as-deposited Al_2O_3/GaN [15]. It is evident from the derived Al_2O_3/GaN band diagram in Ref. [15] that the difference between valence band maxima away from the interface results in a smaller VBO value of 1.2 eV, closer to the values of 0.9 eV [16] and 1 eV [17] reported in the later XPS studies. Duan *et al.* [16] reported that the VBO between Ga-face n-type GaN and ALD Al_2O_3 varies with the thickness of the deposited oxide from 0.9 eV for 4 nm Al_2O_3/GaN to 0.7 eV for 1.3 nm Al_2O_3/GaN. The latter has been explained by an upward energy BB at the GaN surface. Furthermore, Jia *et al*. [17] reported VBO (± 0.2 eV) of 1 eV for ALD Al_2O_3 on non-polar m-plane GaN using angle-resolved (AR)-XPS, where the BEs of Ga 2p and Al 2p CLs at 45° take-off angle (TOA) were used in deriving VBO from Kraut's method.

An AR-XPS experimental study of band alignment of ALD ZrO_2 on undoped GaN on sapphire treated with buffered oxide etchant solution, showed a strong upward band bending at the GaN surface as well as a potential gradiant of 400 meV in the 2 nm ZrO_2 film; the AR-XPS data at 15°, 45° and 75° TOAs have been used with numerical calculations [26] to extract the BE of Ga 3d CL at 0° for the interfacial 2 nm ZrO_2 film on GaN. The VBO value found from Kraut's method is 0.59 eV; with addition of the potential gradient in the oxide film, the VBO shifts to ~1 eV [27]. The theoretically predicted value by Robertson *et al.* [28] is even higher, at 1.6 eV.

In the case of MgO grown by molecular beam epitaxy (MBE) on hydrofluoric acid (HF)-treated n-type GaN, the Ga 3d and Mg 2p XPS CLs were used and Kraut's method applied; the VBO was found to be 1.2 ± 0.2 eV, calculated as an average value measured from three samples

with thicknesses of 4 nm, 7 nm and 10 nm MgO on GaN [29]. A similar value of 1.06 ± 0.15 eV has been reported by Chen *et al.* [30] for radio frequency (RF) plasma asisted MBE MgO on GaN, using the same reference CLs measured at 45° TOA. The more recent XPS study of MBE deposited MgO on GaN [31] revealed a higher VBO of 1.65 eV, the value determined from the three measurements on bulk and interfacial samples using Ga 3s and Mg 2p, as well as Ga 3p and Mg 2p CLs [30]. It is worth noting that neither band bending nor the potential drop across the interfacial oxide layer were discussed in the aforementioned studies, which may significantly alter the band offset values as reported in Refs. [26,32,33].

In this paper, we report band alignment studies of sputtered ZrO_2, Al_2O_3 and MgO on GaN and make comprehensive comparison with the results published in the literature, particularly focusing on band diagrams derived from XPS and Kraut's method. The sputtering technique has been used to deposit the high-k oxides, due to its advantages of low temperature processing, low-cost and the availability of a wider range of materials compared to its ALD counterpart. Sputtered films tend to be amorphous whereas ALD are nanocrystalline. ALD deposited high-k oxides can experience leakage via grain boundaries. Moreover, no band alignment study for sputtered ZrO_2, Al_2O_3 and MgO on GaN has been reported so far. To account for the effect of differential charging [34] and a potentail drop across the oxide film, we have used the method of Iwata *et al.* [35,36] which is based on the extrapolation of the measured BEs to zero oxide thickness and ideally to zero charge. This approach requires that the oxide composition is independent of thickness; hence a set of thin oxide samples (up to 7 nm) on GaN has been processed under identical conditions. Furthermore, AR-XPS was employed to look into the effect of band bending at the interface for all samples. The electrical characterization of the MIS-capacitors fabricated with the gate dielectrics of sputtered ZrO_2, Al_2O_3 and MgO has also been performed.

2. Experimental

2.1. Sample fabrication and cleaning procedure of GaN

The ZrO_2 and Al_2O_3 films were deposited on 5 μm undoped GaN on sapphire, while MgO films were deposited on 2 μm undoped GaN on silicon, using pulsed reactive sputtering (ZrO_2) and RF magnetron sputtering (Al_2O_3, MgO). Prior to oxide deposition, the GaN surface was cleaned using the following sequence: acetone for 10 minutes in an ultrasonic bath, 10 minutes in methanol, 20 minutes in 37 % HCl solution and finally a deionised (DI) water rinse. Our previous

work shows that the HCl treatment is effective in removing oxygen and carbon contaminant on the GaN surface [37] and the organic solvents serve to degrease the surface. For ZrO_2 deposition, the plasma power used was 25 W with oxygen and argon flow rates of 0.6 sccm and 1.4 sccm respectively. The chamber pressure was typically ~1×10^{-3} mbar at room temperature. The sputtering was done with a deposition rate of 0.5 Å/s to deposit the interfacial (3 nm) and bulk (20 nm) ZrO_2/GaN samples respectively. The sputtering power used for Al_2O_3 deposition was 45 W with the rate of 0.06 Å/s to deposit the interfacial (3 nm) and bulk (20 nm) Al_2O_3/GaN samples. For MgO deposition, the sputtering power was 150 W with a chamber pressure of 5 mTorr at room temperature and a rate of 0.04 Å/s to deposit the interfacial (3 nm) and bulk (20 nm) samples.

To account for the effect of differential charging [36,38,39], different batches of interfacial samples were prepared using RF magnetron sputtering. In the case of the oxide/semiconductor heterojunction, the positive charge generated during X-ray bombardment accumulate in the dielectrics forming the heterojunction and induce a strong modification of the kinetic energy of the emitted photoelectron. According to the model in Ref. [34], photoelectrons emitted from the semiconductor are easily compensated by electrons provided through the grounded sample holder. Those originating from the oxide cannot be fully compensated either by electrons tunnelling from the substrate or from stray electrons in the analysis chamber. This phenomenon results in a bending of the valence band (VB) and CL signals in the oxide and affects the accurate evaluation of the VBO. A thickness dependent analysis is needed for the correction of the binding energy of the metallic CL for the interfacial sample to obtain the accurate value of VBO. The plasma power used for ZrO_2 and MgO deposition was 60 W, while for Al_2O_3 it was 45 W with the chamber pressure of 1×10^{-3} mbar at room temperature. The sputtering deposition rate was 0.07 Å/s for the interfacial ZrO_2 and Al_2O_3 samples with thicknesses of 1.9 nm, 3.8 nm and 4.0 nm for the former and 2.5 nm, 4.4 nm and 6.9 nm for the latter oxide measured by Variable Angle Spectroscopic Ellipsometry (VASE) using a Cauchy model [37]. For MgO, the deposition rate of 0.16 Å/s was used to fabricate interfacial samples with thicknesses of 3.4 nm, 5.8 nm and 6.8 nm as measured by VASE. Note that the two sets of samples were sputtered simultaneously in the chamber, one on GaN and a reference one on Si substrate, where the latter was used for VASE measurements to confirm the thickness of deposited films. Room temperature VASE measurements were performed using a J.A. Woollam M2000 ellipsometer with a wavelength range of 241.1–1686.7 nm, which corresponds to an energy range of 0.7–5.2 eV. The measurements were performed at three incident angles of

60°, 65° and 70°, in order to increase the accuracy of the measurements for extracting thickness of the oxide films. The experimental data extracted in the form of two angles (ψ, Δ) vs. photon energy (E) were analysed using Complete EASE software program by developing a theoretical Cauchy model to match the experimental results. The mean squared error (MSE) between the experimental and theoretical (fitted) (ψ, Δ) vs. E curves was in all cases below 5, consistent with a good quality fit of the data.

2.2. XPS measurements

The band alignments of the oxide/GaN interfaces were measured by XPS. The XPS measurements were carried out in a standard ultra-high vacuum (UHV) system with a PSP Vacuum Technology dual anode (Mg/Al) X-ray source and a hemispherical electron energy analyser equipped with five channeltrons. The spectrometer was calibrated using the Ag $3d_{5/2}$ photoelectron line and the Fermi edge from a clean silver foil. The overall resolution of the spectrometer was 0.8 eV and peak positions were determined with a precision of ± 0.05 eV. During all XPS measurements, the X-ray beam exposure was across the whole sample [38,40] to diminish the effect of differential charging when evaluating the VBO. The electron binding energies were corrected using the C 1s peak at 284.6 eV from adventitious surface carbon present in the sputtered films. A Shirley-type background was used for the fitting of all spectra [41]. The measured CL line shapes were fitted using a Voigt function to determine the BE position and full width at half maximum (FWHM) of the peaks. The error bar (± 0.2 eV) in evaluating VBO in this paper is due to valence band maximum determination through the linear interpolation method.

2.3. Device fabrication

Fig. 1 shows the schematic structure of the GaN MIS-capacitor with dielectric layers (ZrO_2 or Al_2O_3 or MgO) and the fabrication flow. The fabrication of MIS-capacitor devices started with the formation of ohmic contacts by electron beam evaporation of Ti/Al/Ni/Au: 20 nm/120 nm/20 nm/45 nm. The samples then underwent rapid thermal annealing (RTA) at 850 °C for 30 seconds in nitrogen (N_2) ambient. The gate dielectrics (ZrO_2, Al_2O_3 and MgO) were sputtered followed by the deposition of the circular gate electrode of Ni/Au: 20 nm/180 nm with the diameter of 100, 120, 140, 160, 180 and 200 μm. The current-voltage (I-V) measurements were performed using an Agilent B1500 semiconductor device analyzer.

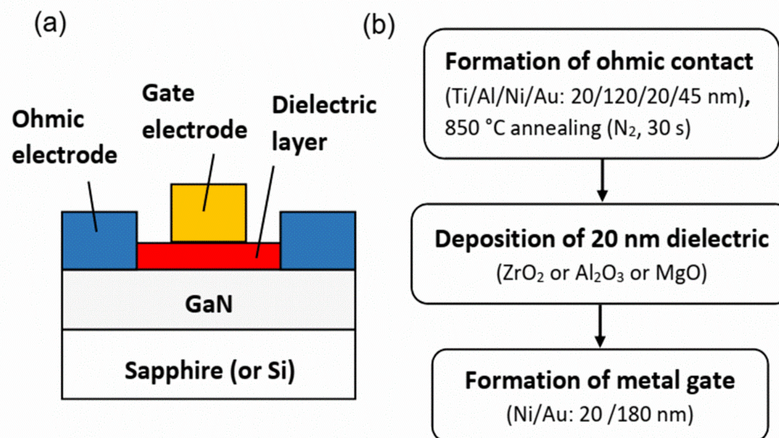

Figure 1. (a) The schematic cross-section and (b) fabrication flow for the GaN MIS-capacitor with dielectric layers (ZrO_2 or Al_2O_3 or MgO).

3. Results and discussion

3.1. Band gap estimation of oxides using XPS O 1s energy loss spectra

The band gap energy values for the dielectric materials were determined using the asymmetry of the O 1s XPS peak, that is the difference between the onsets of energy loss and the O 1s CL [42]. The extracted band gap of ZrO_2 was found to be 5.09 ± 0.2 eV as shown in Fig. 2(a). The latter compares with previously reported values of 5.25 eV from spectroscopic ellipsometry (SE) [43], 5.5 eV from UPS combined with inverse photoemission spectroscopy (IPS) [44], and 5.6 eV from XPS [45]. Moreover, from Figs. 2(b) and (c) the band gaps of Al_2O_3 and MgO were also extracted using the same method and were found to be 6.48 ± 0.2 eV and 7.36 ± 0.2 eV respectively. These values are comparable with previously reported values of 6.4 eV [46,47] from SE; 6.6 eV [17], 6.7 eV [45], 6.8 eV [48,49] from XPS for Al_2O_3 and 7.8 eV [29,31,50] from XPS for MgO. The XPS analysis of the core levels indicates that the sputtered oxides (ZrO_2, Al_2O_3 and MgO) are not fully stoichiometric; for example, quantification from survey spectra showed the metallic (Zr, Al, Mg) to oxygen ratios to be 1:1.9 for ZrO_2, 1:0.95 for MgO and 1:1.3 for Al_2O_3. Furthermore, XPS is a surface sensitive technique and the measurements reflect the topmost few nanometers of the material, which could have defects and contamination. Hence, the reported band gaps may differ from the bulk band gap values reported in the literature.

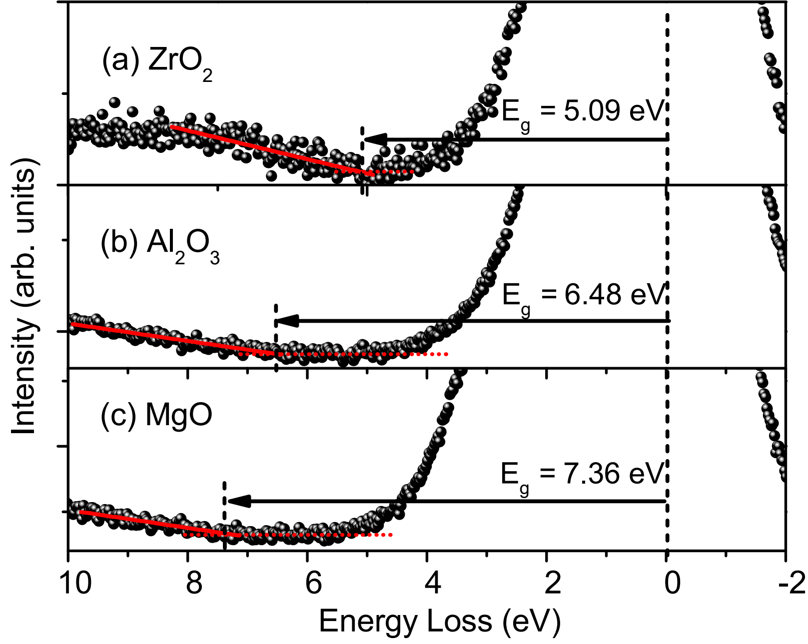

Figure 2. Band gap estimation using XPS O 1s energy loss spectra for sputtered (a) ZrO_2, (b) Al_2O_3 and (c) MgO films.

3.2. Band alignments of ZrO_2, Al_2O_3 and MgO on GaN

In this work, the valence band discontinuity (ΔE_V) or the VBO is extracted using Kraut's method [23] as shown below:

$$\Delta E_V = [E_{CL}^{GaN}(bulk) - E_{VBM}^{GaN}(bulk)] - [E_{CL}^{oxide}(bulk) - E_{VBM}^{oxide}(bulk)] + \Delta E_{CL}, \quad (1)$$

$$\Delta E_{CL} = E_{CL}^{GaN}(interface) - E_{CL}^{oxide}(interface), \quad (2)$$

where $[E_{CL}^{GaN}(bulk) - E_{VBM}^{GaN}(bulk)]$ and $[E_{CL}^{oxide}(bulk) - E_{VBM}^{oxide}(bulk)]$ are the binding energy differences between the chosen reference CLs and their respective valence band maxima for GaN and bulk oxide samples respectively, while ΔE_{CL} is the BE difference of the two chosen CLs for the interfacial sample. The conduction band discontinuity (ΔE_c) or the conduction band offset (CBO) can then be calculated as

$$\Delta E_C = E_g^{oxide} - E_g^{GaN} - \Delta E_V, \quad (3)$$

where E_g^{oxide} and E_g^{GaN} are the band gaps of oxide and GaN substrate, respectively.

Our previously reported value for the band gap of the GaN substrate, that has also been used for sputtered oxides (ZrO_2, Al_2O_3) in this study, is 3.34 ± 0.15 eV obtained from VASE

measurements by linear extrapolation of the leading edge of the imaginary part of the dielectric function, ε_2 vs photon energy spectra to the baseline [37]. This band gap value is used in this study, being in close agreement to the previously reported values of 3.4 eV [29,31,51–53] and 3.44 eV [50].

Fig. 3 depicts measured XPS spectra for the ZrO_2/GaN system, including the Ga 3d CL and VB spectrum for the GaN substrate (Figs. 3(a)-(b)), the Ga 3d and Zr 3d CLs for the interfacial ZrO_2/GaN sample (Figs. 3(c)-(d)), and the Zr 3d CL and VB spectrum for bulk ZrO_2 (Figs. 3(e)-(f)). In the case of the Al_2O_3/GaN and MgO/GaN systems, Al 2p and Mg 2p CLs were measured in combination with Ga 3d from the GaN substrate for estimation of VBO using Kraut's method; the referring XPS spectra for interfacial and bulk oxide samples are shown in Figs. 4(a)-(b) and (e) for Al_2O_3/GaN, and in Figs. 4(c)-(d) and (f) for MgO/GaN. For GaN sample shown in Fig. 3(a), the Ga 3d CL was fitted using two sets of doublet Voigt functions corresponding to Ga-N and Ga-O bonds with spin orbit splitting of 0.45 eV and an area ratio of 0.67 for each doublet [54]. The lower BE side of the main peak at 16.8 eV is attributed to the N 2s component. The most intense peak corresponds to Ga-N $3d_{5/2}$ component at 19.88 eV (Fig. 3(a)) and is chosen as the reference CL for 5 μm GaN on sapphire sample with its respective VBM value of 2.53 ± 0.2 eV (Fig. 3(b)). This gives the $[E_{CL}^{GaN}(bulk) - E_{VBM}^{GaN}(bulk)]$ value of 17.35 eV. This value is in close agreement with the value of 17.34 eV [27] reported for undoped GaN. Partida-Manzanera *et al*. [55] found a $[E_{CL}^{GaN}(bulk) - E_{VBM}^{GaN}(bulk)]$ value of 17.2 eV, slightly smaller as compared to Ye *et al*. [27] and our work, which they attributed to the presence of growth-induced in-plane stress in the nitride epilayer. On the other hand, the $[E_{CL}^{GaN}(bulk) - E_{VBM}^{GaN}(bulk)]$ value of 17.56 eV was obtained for the 2 μm GaN on silicon substrate sample used for sputtering MgO (not shown). This value is in close agreement with experimentally measured values of 17.6 eV [16,29], 17.69 eV [50], 17.7 eV [56] and 17.72 eV [37]. It is worth mentioning that the theoretical value obtained from electronic-state studies of bulk GaN has been found to be in the range of 17.7–17.8 eV [57-58]. It can be noted that the $[E_{CL}^{GaN}(bulk) - E_{VBM}^{GaN}(bulk)]$ values differ in the two GaN samples used in this study. While the values are within the range reported in the literature, the discrepancy could be attributed to differences in the surface conditions of two samples. Note that the VBM for the two GaN samples is found to be 2.5 ± 0.2 eV. Since the BEs in XPS are measured with respect to the Fermi level of the spectrometer that corresponds to the position of the Fermi level within the band gap of the semiconductor, the extrapolated value of the VBM indicates that the Fermi level is

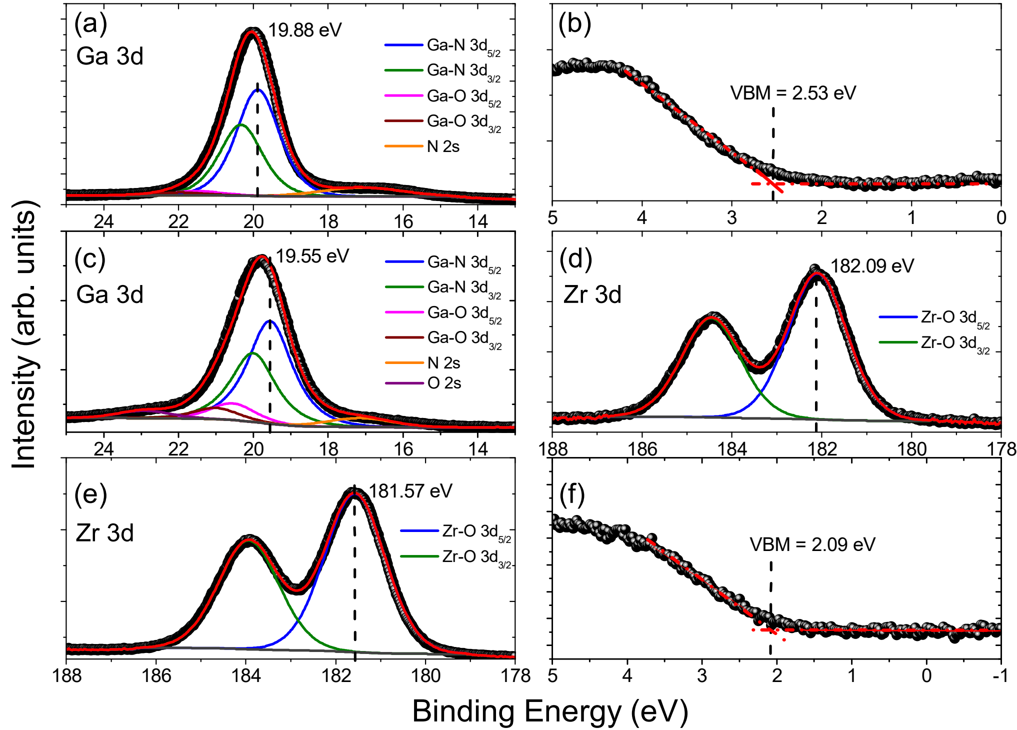

Figure 3. The XPS spectra of (a) Ga 3d CL and (b) valence band spectrum for 5 µm GaN on sapphire; (c) Ga 3d and (d) Zr 3d CLs for interfacial ZrO_2/GaN sample; (e) the Zr 3d CL and (f) valence band spectrum showing VBM extraction for bulk ZrO_2/GaN sample.

closer to the conduction band (CB) edge. It has been shown that undoped GaN can exhibit unintentional n-type conductivity [59]. Furthermore, this could also indicate downward band bending and an accumulated GaN surface for both substrate samples used in this work. In a recent study, a downward bend bending has been reported for GaN samples degreased for 5 minutes in acetone, followed by immersion in isopropyl alcohol and a rinse in flowing DI water, without using HF [60]. In our work, GaN samples were also cleaned without HF. The observation of an accumulated GaN surface has been explained by a significant positive charge density residing within the native oxide [60-61]. It has been suggested that the positive charges on GaN surface compensate the polarization-induced negative surface charge and form an electron accumulation layer. With an accumulated surface, the Fermi level is situated close to the GaN conduction band edge and thus the positive charges cannot be attributed to donor-like gap states [61]. A possible source for the positive charge may be (i) interfacial fixed charge with energy states between the conduction band minima of the native oxide and GaN [61]; or (ii) a possible polarity inversion of

the GaN surface, that is a change in the spontaneous polarization charge from negative to positive due to the formation of Ga-O bonds. It can be seen from Figs. 3(a), 3(c), 4(a) and 4(c) that there are Ga-O bonds on the higher BE side of Ga 3d CL peak, which could underpin the existence of a thin GaO_x layer, and a presence of positive charges on the GaN surface.

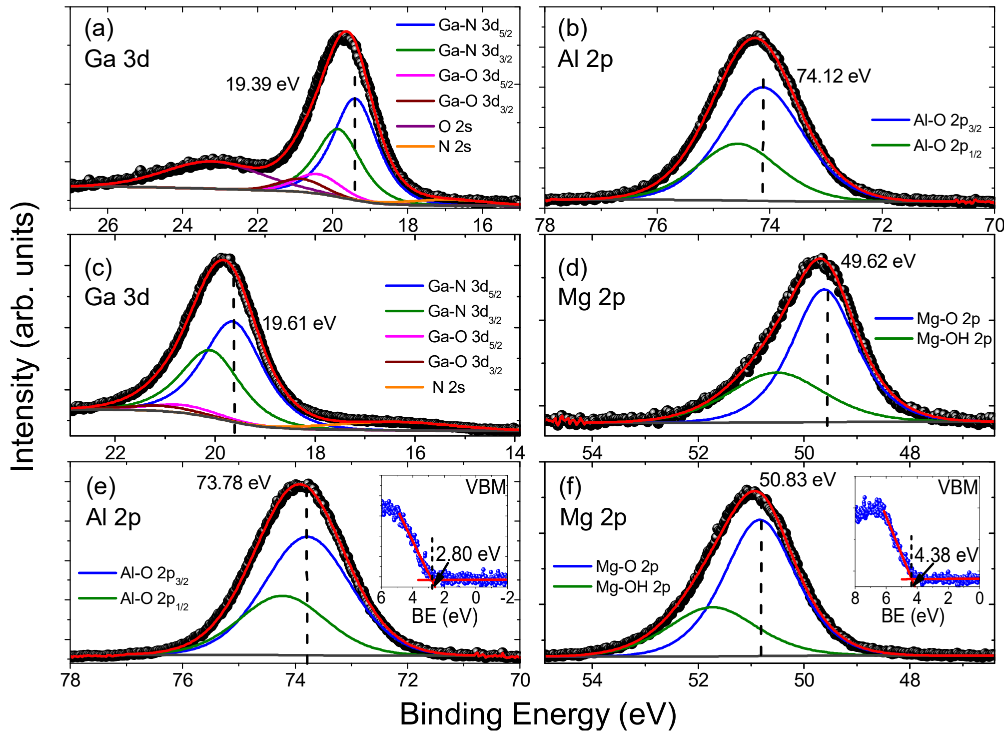

Figure 4. The XPS spectra for (a) Ga 3d, (b) Al 2p CLs for interfacial Al_2O_3/GaN; (c) Ga 3d and (d) Mg 2p CLs for interfacial MgO/GaN; (e) Al 2p and Mg 2p CLs for bulk Al_2O_3 and MgO films. The insets in both (e) and (f) refer to VB spectra and extraction of VBM for both bulk oxide films.

Figs. 3(c) and (d) show XPS spectra for the interfacial ZrO_2/GaN sample, where the Ga 3d CL was fitted using two doublet Voigt function related to Ga-N and Ga-O bonds, N 2s, and O 2s components, whereas the Zr 3d CL was fitted with a single doublet Voigt function related to Zr-O bond. The peak positions at BEs of 19.55 eV (Fig. 3(c)) and 182.09 eV (Fig. 3(d)) corresponding to Ga-N $3d_{5/2}$ and Zr-O $3d_{5/2}$ respectively were selected as reference CLs. For the bulk ZrO_2 sample, the peak position of Zr-O $3d_{5/2}$ at 181.57 eV (Fig. 3(e)) is chosen as the reference CL with its respective VBM value of 2.09 eV (Fig. 3(e)), giving $[E_{CL}^{oxide}(bulk) - E_{VBM}^{oxide}(bulk)]$ = 179.48 eV. In a similar way, Ga 3d and Al 2p XPS CLs were designated and fitted in Figs. 4(a)-(b) for Al_2O_3/GaN, as well as Ga 3d and Mg 2p for MgO/GaN as shown in Figs. 4(c)-(d). The high

resolution spectra of the VB region for bulk Al_2O_3 and MgO are shown in the insets of Figs. 4(e) and (f) respectively, with extrapolated values of the VBM of 2.80 eV for Al_2O_3 and 4.38 eV for MgO. The resultant $[E_{CL}^{oxide}(bulk) - E_{VBM}^{oxide}(bulk)]$ values are 70.98 eV and 46.45 eV for Al_2O_3 and MgO respectively.

The effect of differential charging can be seen in Figs. 5(a)-(c) and Table I. The constant value of the BE of Zr 3d CL of 182.1 ± 0.1 eV in ZrO_2/GaN heterostructures with all thicknesses in Fig. 5(a) can be interpreted as evidence that no charge accumulation occurs in the oxide films during the X-ray irradiation. The ΔE_{CL} values from thin ZrO_2/GaN samples are listed in Table I, using Eq. (1), the VBO is calculated to vary between 0.29 eV to 0.41 eV, giving an average value of 0.35 ± 0.1 eV. In the Al_2O_3/GaN (Fig. 5(b)) and MgO/GaN (Fig. 5(c)) heterojunctions, the Al 2p and Mg 2p CLs exhibit a very small increasing shift towards higher BEs when increasing Al_2O_3 and MgO film thicknesses, thus providing clear fingerprints of a small charging phenomenon. In all cases, a constant energy difference between the metallic (M) Zr 3d, Al 2p and Mg 2p CL and O 1s was observed (± 0.2 eV) regardless of the thickness of the oxide films (see Table I). This suggests that no chemical modification of the oxide matrix occurred when increasing the thickness of the deposited oxide. From the linear fit of the experimental data in Figs. 5(b) and (c), the BEs of the Al 2p and Mg 2p CLs in the interfacial Al_2O_3/GaN and MgO/GaN are extrapolated to zero oxide thickness, and found to be 74.48 eV and 49.70 eV, respectively. The ΔE_{CL} values for Al_2O_3/GaN and MgO/GaN are listed in Table I, and using Eq. (1), the average VBOs are found to be 1.07 ± 0.1 eV for Al_2O_3/GaN and 1.19 ± 0.1 eV for MgO/GaN.

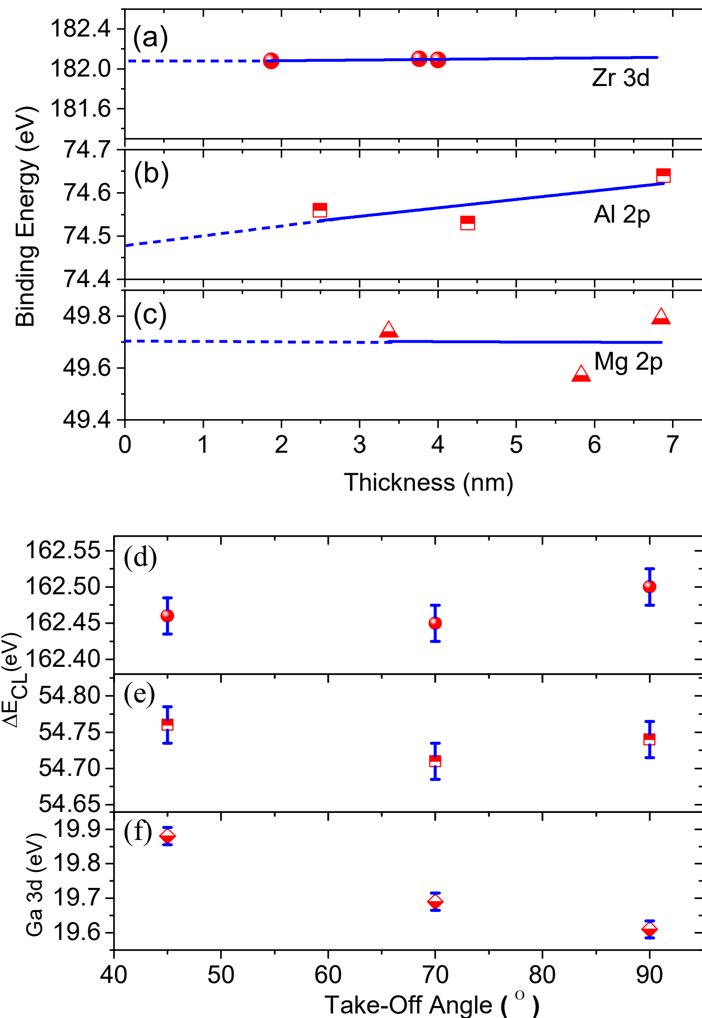

Figure 5. The binding energy of (a) Zr 3d, (b) Al 2p, (c) Mg 2p measured for a range of thin (up to 7 nm) oxide/GaN samples. A small differential charging effect can be seen in (b) and (c) for A_2O_3 and MgO respectively. The CL difference, ΔE_{CL} (eV) between (d) Zr 3d and Ga 3d and (e) Al 2p and Ga 3d for thin (3 nm nominal) ZrO_2/GaN and Al_2O_3/GaN samples as a function of XPS take-off angle. (f) The variation of Ga 3d CL for thin (3 nm nominal) MgO/GaN sample vs. XPS take-off angle.

Table I A summary of VBO results obtained from a set of interfacial oxide/GaN samples with thickness of the oxides measured by VASE; ΔE_{CL} is the difference in binding energies between metallic (M) and Ga 3d XPS CLs, while ΔM-O 1s is the BE difference between the metallic and O 1s XPS CLs. M refers to Zr 3d, Al 2p and Mg 2p for respective ZrO_2, Al_2O_3 and MgO on GaN. The average VBO value across the three films is given on the right-hand side of VBO column.

	Thickness (nm)	ΔE_{CL} (eV)	ΔM-O 1s (eV)	VBO (eV)	
ZrO_2/GaN	1.9	162.42	348.10	0.29	
	3.8	162.46	348.05	0.33	0.35 ± 0.1
	4.0	162.54	348.01	0.41	
Al_2O_3/GaN	2.5	54.60	456.84	0.97	
	4.4	54.79	456.85	1.16	1.07 ± 0.1
	6.9	54.78	456.81	1.15	
MgO/GaN	3.4	30.08	481.76	1.19	
	5.8	30.09	481.86	1.20	1.19 ± 0.1
	6.8	30.07	481.67	1.18	

Furthermore, we looked into the effect of band bending at the oxide/GaN interface by monitoring the difference in BEs of Ga 3d and metallic CLs by AR-XPS as shown in Figs. 5(d)-(e). It can be seen that ΔE_{CL} is within 0.1 eV for both ZrO_2/GaN and Al_2O_3/GaN, indicating negligable BB for TOAs up to 45°. Using the Eq. (1) and the values of ΔE_{CL} from Figs. 5(d)-(e), the VBO was found to be 0.37 eV, 0.32 eV to 0.33 eV for ZrO_2/GaN; and 1.11 eV, 1.08 eV and 1.13 eV for Al_2O_3/GaN when TOA varies from 90°, 70° to 45° respectively. Since, the Ga 3d CLs for all three interfacial ZrO_2/GaN (Fig. 3(c)), Al_2O_3/GaN (Fig. 4(a)) and MgO/GaN (Fig. 4(c)) shift towards lower binding energies in comparison to the GaN, this means that there is an upward bend bending after oxide deposition; since the GaN surface is accumulated (see Fig. 6(a)), this results in less downward BB at the oxide/GaN interface. The latter can be underpinned by smaller values of the VB edge from the Fermi level at the interface, that is deduced from the measured Ga 3d CL binding energy and measured $[E_{CL}^{GaN}(bulk) - E_{VBM}^{GaN}(bulk)]$ i.e. for ZrO_2 this is 19.55 eV – 17.35 eV = 2.2 eV; for Al_2O_3 (Fig. 4(a)) 19.39 eV -17.35 eV = 2.04 eV; for MgO (Fig. 4(c)) 19.61 eV – 17.56 eV = 2.05 eV (Fig. 6(b)). Note that due to the very small photoionisation cross-section of Mg 2p (0.005), the angle-resolved data could not be recorded; instead only Ga 3d CL is

measured by AR-XPS. In Fig. 5(f), the BE of Ga $3d_{5/2}$ CL for MgO/GaN sample is seen to increase from 19.61 eV at 90° TOA to 19.88 eV at 45° TOA. The latter is in agreement with a small downward band bending of up to 0.3 eV for MgO/GaN, as found observing the VB edge position from the Fermi level at the interface.

A summary of all measured XPS CL differences, band gap, VBO and CBO extracted in this work and their comparison with literature values is given in Table II. The calculated VBOs (± 0.2 eV) using Eqs. (1) and (2) for ZrO_2, Al_2O_3 and MgO on GaN are found to be 0.4 eV, 1.1 eV and 1.2 eV with corresponding CBOs (± 0.2 eV) calculated from Eq. (3), of 1.3 eV, 2.0 eV and 2.8 eV respectively. The band offset values based on the charge-corrected ΔE_{CL} are summarized in Table II. The band diagrams for the ZrO_2, Al_2O_3 and MgO on GaN are shown in Fig. 6(b). In terms of band gap values, we can infer smaller band gap values of 5.1 eV for ZrO_2 and 7.4 eV for MgO than those reported in the literature measured by XPS as listed in Table II. The smaller band gap values measured in this work could be due to the non-stoichiometric surface of sputtered ZrO_2 and MgO films. For Al_2O_3, our XPS derived band gap value of 6.48 eV is in close agreement with our previously reported value of 6.43 eV by vacuum ultra violet (VUV)-VASE [39] on MBE-deposited Al_2O_3, as well as the most recent theoretically predicted value of 6.36 eV [62]. A variation of reported band gap values for Al_2O_3 can be seen in Table II, from 6.4 eV to 6.9 eV.

Table II The measured values of difference in CLs, E_g, VBO and CBO from this work (± 0.2 eV) compared to literature values.

Material System	$E_{CL}^{GaN} - E_{VBM}^{GaN}$ (eV)	$E_{CL}^{oxide} - E_{VBM}^{oxide}$ (eV)	ΔE_{CL} (eV)	E_g (eV)	VBO (eV)	CBO (eV)
ZrO_2/GaN	17.35 17.34 [27]	179.48 179.43 [27]	162.54 162.68 [27]	5.09 5.25 [43] 5.5 [44] 5.6 [45]	0.4 1 [27] 1.6 [28]	1.3 1.2 [27] 1.1 [28]
Al_2O_3/GaN	17.35 17.8 [15,63] 17.6 [16,29] 17.7 [56]	70.98 70.4 [15] 71.8 [16] 70.6 [63]	54.74 54.4 [15] 55.1 [16] 54.9 [63]	6.48 6.6 [17] 6.7 [45] 6.77 [50] 6.8 [49] 6.4 [39,46,62] 7.6 [56]	1.1 1.8 [15] 0.9 [16] 1.0 [17] 2.1 [28] 1.5 [56] 2.0 [63] 1.17 [62]	2.0 1.3 [15,63] 2.2 [17] 3.4 [28] 2.7 [56] 1.79 [62]
MgO/GaN	17.56 17.6 [16,29] 17.69 [50] 17.72 [37]	46.45 46.79 [29] 46.94 [50]	30.09 30.32 [29] 30.31 [50]	7.36 7.8 [29,31,50]	1.2 1.2 [29] 1.65 [31] 1.06 [50]	2.8 3.2 [29] 2.75 [31] 2.6 [28] 3.3 [50]

[15–17,27,29,31,37,45,48–50,63]XPS [56]photoemission spectroscopy and XAS [44]UPS and IPS [43,46]SE [50][39]photoluminescence [28,62]theoretical CNL method

The VBO results indicate a smaller value of 0.4 ± 0.2 eV for sputtered ZrO_2 on GaN than the previously reported value of 1 eV for ALD deposited ZrO_2 on GaN [27], while the CBO of 1.3 ± 0.2 eV is within the measurement error to the values of 1.2 eV [27] and the theoretically predicted value of 1.1 eV [28]. The difference in CL values in our work is comparable with Ye *et al*. [27] (see Table II), but the discrepancy is mainly due to a potential gradient in the ZrO_2 layer and a strong upward BB at the GaN surface. The value of VBO of 1.1 eV ± 0.2 eV for Al_2O_3/GaN from our work is in agreement with the experimental derived values of 0.9 eV [16] and 1.0 eV [17] for conventional ALD Al_2O_3 on HF-treated GaN. Furthermore, it shows excellent agreement with the most recent published theoretical VBO and CBO values of 1.17 eV and 1.79 eV respectively [62]. It is worth mentioning that earlier theoretical work by the same group [28] predicted much higher VBO values for both ZrO_2/GaN and Al_2O_3/GaN. The discrepancy of up to 1 eV of VBO compared to the work of Yang *et al*. [15,63] is due to a BE difference in the Al 2p CL with respect to Ga 3d

CL and between Ga 3d CL and VBM. These discrepancies could be the result of different cleaning and deposition processes, namely plasma enhanced-ALD deposited Al_2O_3 on HCl and H_2/N_2 plasma-treated GaN [15] or on NH_4OH and NH_3 plasma-treated GaN [63]. Both these processes could result in a strong upward band bending at the oxide/GaN interface and higher VBOs of 1.8 eV [15] and 2.0 eV [63] (Table II). Furthermore, Toyoda *et al*. [56] have measured a VBO of 1.5 eV for chemical vapour deposited Al_2O_3/n-GaN using VB spectra of Al_2O_3 films on GaN normalized by that of a bare GaN layer. In the case of MgO/GaN, our measured VBO of 1.2 ± 0.2 eV is in agreement with the experimentally derived values of 1.2 eV [38] and 1.06 eV [50] for MgO grown by MBE and RF plasma assisted MBE on untreated GaN respectively. Note that a larger VBO of 1.65 eV has been reported using Kraut's method, however no charge-correction in the oxide film nor BB at the GaN surface have been taken into account [31]. The CBO of MgO/GaN of 2.8 ± 0.2 eV is within measurement error with the experimental value of 2.75 eV [31] and theoretically predicted value of 2.6 eV [28] as shown in Table II.

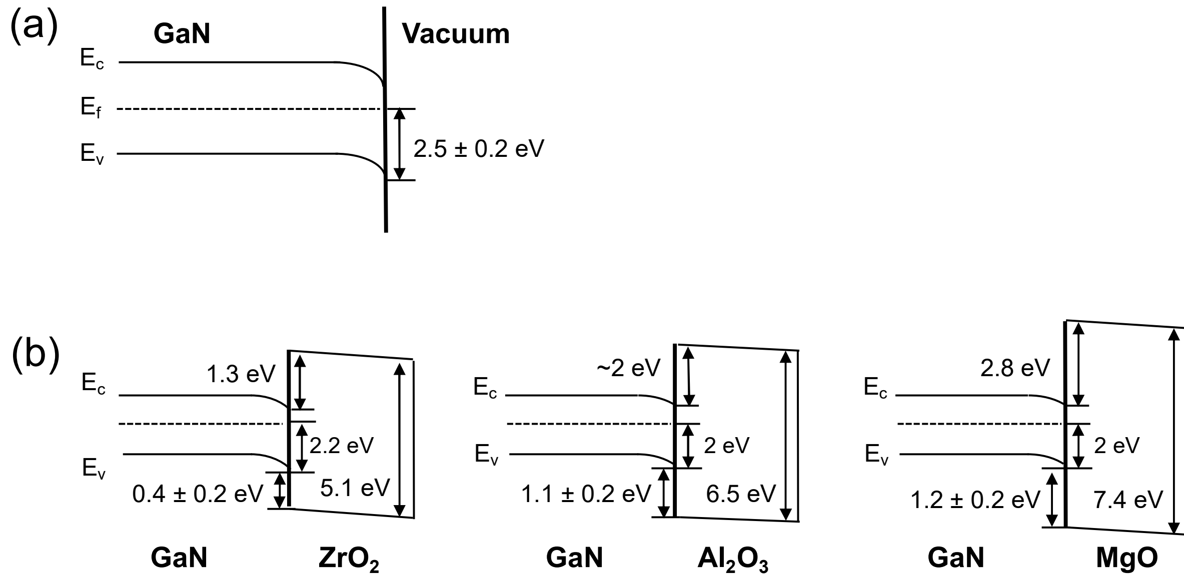

Figure 6. The schematics of XPS experimentally derived band alignments: (a) at GaN surface; (b) for ZrO_2/GaN, Al_2O_3/GaN and MgO/GaN fabricated in this work by sputtering. (The diagrams are not to scale.)

3.3. Electrical characterization

The I-V and current density-voltage (J-V) characteristics of MIS-capacitors fabricated using the three different dielectrics are shown in Fig. 7. The leakage current density of MIS-capacitor

with 20 nm ZrO_2 gate dielectric is 6.2 $\times 10^{-4}$ A/cm^2 at 1 V, which, taking into account the difference in oxide thickness, is lower than the previously reported value of 0.88 A/cm^2 at 1 V for 4.4 nm ALD-deposited ZrO_2/GaN MIS-capacitor [64]. Similarly, the 20 nm Al_2O_3-based MIS-capacitor shows a lower leakage current density than that of ZrO_2 at 5.3 $\times 10^{-6}$ A/cm^2 at 1 V gate bias. A value of 1×10^{-4} A/cm^2 at –10 V was reported for 25 nm Al_2O_3 on HF treated GaN deposited by ALD [17] and 5.33×10^{-2} A/cm^2 at 4 V for the ALD-deposited 14 nm Al_2O_3 on a HCl treated GaN substrate [65]. The leakage current density for the 20 nm MgO MIS-capacitor is 3.2 $\times 10^{-6}$ A/cm^2 at 1 V. A value of 5 $\times 10^{-3}$ A/cm^2 for 80 nm MgO in GaN MIS-FET (Field Effect Transistor) device at 2.2 V has been reported [66]. Direct comparisons with the literature are problematic due to the different oxide thicknesses but considering the trends in the scaling of SiO_2, our oxides can be considered relatively low leakage. It is critically important that a gate dielectric has sufficient band offsets of at least 1 eV to ensure that carriers are confined mainly within the channel. The band offsets affect the gate leakage current with an exponential relationship. In our work, MgO exhibits the lowest leakage current density with the highest VBO and CBO of 1.2 eV and 2.8 eV respectively, whereas ZrO_2-based devices have the highest leakage current density corresponding to VBO and CBO of 0.4 eV and 1.3 eV, respectively. Note that the referenced papers lack analysis of the leakage current data. A weak temperature dependence was noted for the oxide leakage in ALD deposited ZrO_2 on GaN [64] indicating the dominance of a tunnelling mechanism but a barrier height (conduction band offset) was not extracted. The band offset values (VBO = 1 eV and CBO = 2.2 eV) obtained by Jia *et al*. [17] are comparable with this work (VBO = 1.1 eV and CBO = 2.2 eV) but the differing test conditions make it difficult to compare leakage currents directly. Wei *et al.* [65] , Irokawa *et al.* [66] and Kim *et al.* [67] report leakage currents similar to those of this work, but did not investigate conduction mechanisms or extract band offset(s). Finally it is important to note that further analysis of our results (not shown) using typical J-V characteristics plotted on log-log scales shows evidence of the space-charge-limited (SCL) conduction mechanism in the low electric field region (0-1.5 V) which could indicate that the current flow is inhomogeneous and bulk rather than electrode limited. It is not possible therefore, to extract barrier heights which might be compared to those derived from XPS. Presentation of the full details of the analysis serves no useful purpose for the overall conclusions of the paper and is not presented here.

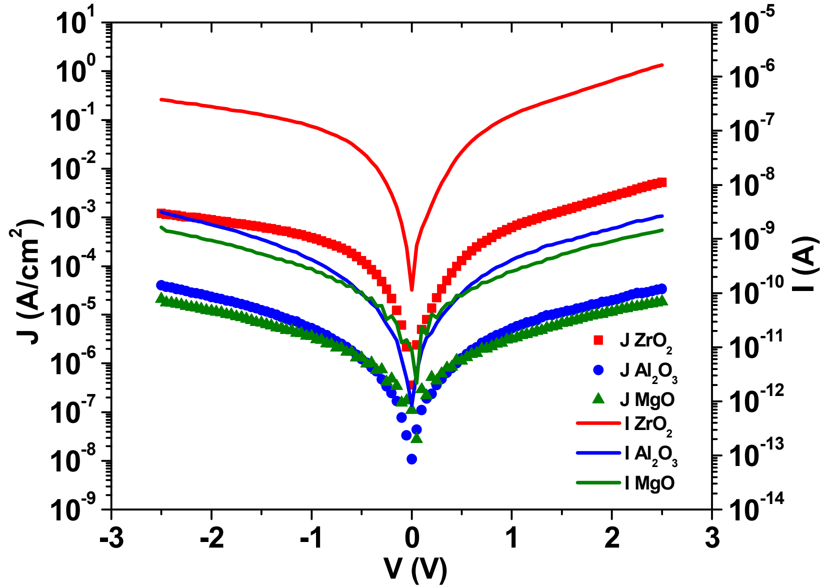

Figure 7. The J-V and I-V curves for MIS-capacitors on GaN with three different gate dielectrics (ZrO_2, Al_2O_3, MgO) deposited by sputtering. The measured circular device areas are 7.85 nm^2 for GaN MIS-capacitor with gate dielectrics Al_2O_3 and MgO, while 31.4 nm^2 for ZrO_2.

4. Conclusion

The band gap and valence band offsets of sputtered ZrO_2, Al_2O_3 and MgO on GaN have been measured experimentally using XPS. The valence band offsets (± 0.2 eV) for ZrO_2, Al_2O_3 and MgO on GaN using Kraut's method and charge corrected ΔE_{CL} were found to be 0.4 eV, 1.1 eV and 1.2 eV respectively. The XPS O 1s loss spectroscopy was used to determine the band gaps (± 0.2 eV) of ZrO_2 (5.1 eV), Al_2O_3 (6.5 eV) and MgO (7.4 eV). The angle-resolved XPS data indicate a small downward band bending for all oxide/GaN interfaces. The electrical characterization of MIS-capacitors with different gate dielectrics (ZrO_2, Al_2O_3 and MgO) has also been performed. The J-V characteristics of MIS-capacitors with gate dielectrics MgO and Al_2O_3 show low leakage current of 3.2×10^{-6} A/cm^2 and 5.6×10^{-6} A/cm^2 respectively at a positive bias of 1 V, whereas, a high leakage current of 6.2×10^{-4} A/cm^2 at 1 V is observed for the MIS-capacitor with ZrO_2 gate dielectric. The results are of significance for future GaN-based HEMT device design.

Acknowledgements

The work was conducted under the University Grants Commission – UK-India Education Research Initiative (UGC-UKIERI) joint research programme UKIERI III, project numbers IND/CONT/G/17-18/18 and F.No.184-1/2018(IC), titled "Dielectric engineering on GaN for

sustainable energy applications" funded by the British Council. The authors also acknowledge UKRI GCRF GIAA award 2018/19 and 'Digital in India' project no. EP/P510981/1, both funded by the EPSRC, UK. S.N. Supardan would like to acknowledge the Malaysia Ministry of Higher Education and Universiti Teknologi MARA (UiTM), Malaysia for financial support. Dr. A.P. Shaw is acknowledged for the deposition of Al_2O_3.

References

[1] Amano H *et al* 2018 *J. Phys. D: Appl. Phys.* **51** 163001

[2] Chen K J, Häberlen O, Lidow A, Tsai C L, Ueda T, Uemoto Y and Wu Y 2017 *IEEE Trans. Electron Devices* **64** 779-795

[3] Wong K R *et al* 2015 A next generation CMOS-compatible GaN-on-Si transistors for high efficiency energy systems *IEEE Int. Electron Devices Meeting* pp 9.5.1-9.5.4

[4] Oka T and Nozawa T 2008 *IEEE Electron Device Lett.* **29** 668

[5] Ozbek A M and Baliga B J 2011 *IEEE Electron Device Lett.* **32** 1361

[6] Turuvekere S, Karumuri N, Rahman A A, Bhattacharya A, Dasgupta A and Dasgupta N 2013 *IEEE Trans. Electron Devices* **60** 3157

[7] Gregušová D *et al* 2014 *Appl. Phys. Lett.* **104** 013506

[8] Hao R *et al* 2017 *IEEE Electron Device Lett.* **38** 1567

[9] Shin B, Weber J R, Long R D, Hurley P K, Van De Walle C G and McIntyre P C 2010 *Appl. Phys. Lett.* **96** 152908

[10] Hashizume T, Ootomo S and Hasegawa H 2003 *Appl. Phys. Lett.* **83** 2952

[11] Jiang H, Liu C, Chen Y, Lu X, Tang C W and Lau K M 2017 *IEEE Trans. Electron Devices* **64** 832–839

[12] Lu X, Yu K, Jiang H, Zhang A and Lau K M 2017 *IEEE Trans. Electron Devices* **64** 824–831

[13] Liu X *et al* 2018 *ACS Appl. Mater. Interfaces* **10** 21721

[14] Čičo K, Gregušová D, Kuzmík J, Jurkovič M, Alexewicz A, Di Forte Poisson M A, Pogany D, Strasser G, Delage S and Fröhlich K 2012 *Solid. State. Electron.* **67** 74

[15] Yang J, Eller B S, Zhu C, England C and Nemanich R J 2012 *J. Appl. Phys.* **112** 053710

[16] Duan T L, Pan J S and Ang D S 2013 *Appl. Phys. Lett.* **102** 201604

[17] Jia Y, Wallace J S, Echeverria E, Jr. Gardella J A and Singisetti U 2017 *Phys. Status Solidi B* **254** 1600681

[18] Wu Y Q, Shen T, Ye P D and Wilk G D 2007 *Appl. Phys. Lett.* **90** 143504

[19] He G, Gao J, Chen H, Cui J, Sun Z and Chen X 2014 *ACS Appl. Mater. Interfaces* **6** 22013

[20] He G, Liu J, Chen H, Liu Y, Sun Z, Chen X, Liud M and Zhang L 2014 *J. Mater. Chem. C* **2** 5299

[21] He G, Chen X and Sun Z 2013 *Surface Science Reports* **68** 68

[22] Zhang J W, He G, Zhou L, Chen H S, Chen X S, Chen X F, Deng B, Lv J G and Sun Z 2014 *J. Alloys and Compounds* **611** 253

[23] Kraut E A, Grant R W, Waldrop J R and Kowalczyk S P 1983 *Phys. Rev. B* **28** 1965

[24] Ganguly S, Verma J, Li G, Zimmermann T, Xing H and Jena D 2014 *Appl. Phys. Lett.* **99** 193504

[25] Cook Jr. T E, Fulton C C, Mecouch W J, Davis R F, Lucovsky G and Nemanich R J 2003 *J. Appl. Phys.* **94** 7155

[26] Akazawa M, Gao B, Hashizume T, Hiroki M, Yamahata S and Shigekawa N 2011 *J. Appl. Phys.* **109** 013703

[27] Ye G, Wang H, Arulkumaran S, Ng G I, Li Y, Liu Z H and Ang K S 2014 *Appl. Phys. Lett.* **105** 022106

[28] Robertson J and Falabretti B 2006 *J. Appl. Phys.* **100** 014111

[29] Craft H S, Collazo R, Losego M D, Mita S, Sitar Z and Maria J P 2007 *J. Appl. Phys.* **102** 074104

[30] Chen J J, Gila B P, Hlad M, Gerger A, Ren F, Abernathy C R and Pearton S J 2006 *Appl. Phys. Lett.* **88** 042113

[31] Paisley E A, Brumbach M, Allerman A A, Atcitty S, Baca A G, Armstrong A M, Kaplar R J and Ihlefeld J F 2015 *Appl. Phys. Lett.* **107** 102101

[32] Xu X, Liu X, Guo Y, Wang J, Song H, Yang S, Wei H, Zhu Q and Wang Z 2010 *J. Appl. Phys.* **107** 104510

[33] Zhang K, Liao M, Sumiya M, Koide Y and Sang L 2016 *J. Appl. Phys.* **120** 185305

[34] Alay J L and Hirose M 1997 *J. Appl. Phys.* **81** 1606

[35] Iwata S and Ishizaka A 1996 *Appl. Phys. Rev.* **79** 6653

[36] Perego M, Molle A and Seguini G 2012 *Appl. Phys. Lett.* **101** 211606

[37] Sawangsri K *et al* 2017 *Microelectron. Eng.* **178** 178

[38] Perego M and Seguini G 2011 *J. Appl. Phys.* **110** 053711

[39] Mitrovic I Z *et al* 2015 *J. Appl. Phys.* **117** 214104

[40] Bersch E, Di M, Consiglio S, Clark R D, Leusink G J and Diebold A C 2010 *J. Appl. Phys.* **107** 043702

[41] Shirley D A 1972 *Phys. Rev. B* **5** 4709

[42] Yu H Y, Li M F, Cho B J, Yeo C C, Joo M S, Kwong D-L, Pan J S, Ang C H, Zheng J Z and Ramanathan S 2002 *Appl. Phys. Lett.* **81** 376

[43] Zhu L Q, Fang Q, He G, Liu M, Xu X X and Zhang L D 2006 *Mater. Sci. Semicond. Process.* **9** 1025

[44] Bersch E, Rangan S, Bartynski R A, Garfunkel E and Vescovo E 2008 *Phys. Rev. B* **78** 085114

[45] Nohira H *et al* 2002 *J. Non. Cryst. Solids* **303** 83

[46] Nguyen N V *et al* 2008 *Appl. Phys. Lett.* **93** 082105

[47] Mitrovic I Z *et al* 2014 *J. Appl. Phys.* **115** 114102

[48] Huang M L, Chang Y C, Chang Y H, Lin T D, Kwo J and Hong M 2009 *Appl. Phys. Lett.* **94** 052106

[49] Kamimura T, Sasaki K, Wong M H, Krishnamurthy D, Kuramata A, Masui T, Yamakoshi S and Higashiwaki M 2014 *Appl. Phys. Lett.* **104** 192104

[50] Chen J, Gila B P, Hlad M, Gerger A, Ren F, Abernathy C R and Pearton S J 2006 *Appl. Phys. Lett.* **88** 042113

[51] Muth J F, Lee J H, Shmagin I K, Kolbas R M, Casey H C, Keller B P, Mishra U K and DenBaars S P 1997 *Appl. Phys. Lett.* **71** 2572

[52] Kim T J, Byun J S, Kim Y D, Kim H and Chang Y C 2008 *J. Korean Phys. Soc.* **53** 1575

[53] Wagner J, Obloh H, Kunzer M, Maier M, Köhler K and Johs B 2001 *J. Appl. Phys.* **89** 2779

[54] Wagner C D, Naumkin A V, Kraut V A, Allison J W, Powell C J and Rumble J R 2004 *NIST Standard Reference Database 20 version 3.4 (Web Version)*

[55] Partida M T, Roberts J W, Bhat T N, Zhang Z, Tan H R, Dolmanan S B, Sedghi N, Tripathy S and Potter R J 2016 *J. Appl. Phys.* **119** 025303

[56] Toyoda S, Shinohara T, Kumigashira H, Oshima M and Kato Y 2012 *Appl. Phys. Lett.* **101** 231607

[57] Cook Jr. T E, Fulton C C, Mecouch W J, Davis R F, Lucovsky G and Nemanich R J 2003 *J. Appl .Phys.* **94** 7155

[58] Waldrop J R and Grant R W 1996 *Appl. Phys. Lett.* **68** 2879

[59] Saarinen K *et al* 1999 *Phys. B* **273-274** 33

[60] Duan T L, Pan J S and Ang D S 2016 *ECS J. Solid State Sci. Technol.* **5** P514

[61] Esposto M, Krishnamoorthy S, Nath D N, Bajaj S, Hung T H and Rajan S 2011 *Appl. Phys. Lett.* **99** 133503

[62] Zhaofu Z, Guo Y and Robertson J 2019 *Appl. Phys. Express* **114** 161601

[63] Yang J, Eller B S and Nemanich R J 2014 *J. Appl. Phys.* **116** 123702

[64] Hauff P Von, Afshar A, Bothe K, Cadien K and Barlage D 2013 *Appl. Phys. Lett.* **102** 251601

[65] Wei D, Hossain T, Briggs D P and Edgar J H 2014 *ECS J. of Solid State Sci. Technol.* **3** N127

[66] Irokawa Y *et al* 2004 *Appl. Phys. Lett.* **84** 2919

[67] Kim J *et al* 2002 *J. Electrochem. Soc.* **149** G482